Iminophosphorane-substituted Proton Sponges. Part 1. X-Ray Molecular Structures of 1,8-Diaminonaphthalene and 1-Amino-8-triphenylphosphoranylideneaminonaphthalene

Antonio L. Llamas-Saiz,[a] Concepción Foces-Foces,*[a] Pedro Molina,*[b] Mateo Alajarin,[b] Angel Vidal,[b] Rosa M. Claramunt[c] and José Elguero*[c]
[a] *UEI de Cristalografía, Instituto de Química-Física 'Rocasolano', CSIC, Serrano, 119, 28006 Madrid, Spain*
[b] *Departamento de Química Orgánica, Facultad de Ciencias, Campus Universitario de Espinardo, 30071 Murcia, Spain*
[c] *Departamento de Química Orgánica, Facultad de Ciencias, UNED, Ciudad Universitaria, 28040 Madrid*

The molecular structures of 1,8-diaminonaphthalene (**1**) and 1-amino-8-triphenylphosphoranylideneaminonaphthalene·0.5 C_6H_6 (**2**) have been solved by X-ray crystallography. The benzene guest molecule is discussed in relation to the host matrix hole in which it is included. The molecular structure of compound **1** has been compared with the results of a theoretical analysis at the AM1 level. The complete potential-energy surface, as a function of the conformation of both NH_2 groups (ϕ_1, ϕ_2), has also been calculated. The absolute minimum ($\phi_1 = \phi_2 = 47.0°$) is very close to the experimental geometries of the two independent molecules of compound **1**.

'Proton sponges'—aromatic nitrogen compounds with exceptional basicities—[1] are commonly associated with 1,8-bis(dimethylamino)naphthalene (Scheme 1). This basic structure has been modified in two main ways. First, the naphthalene ring has been replaced by other aromatic rings, such as fluorene,[1] phenanthrene[1] or dibenzothiophene.[2] Secondly, the dimethylamino group has been replaced by a pyridine-like nitrogen, as in quinolino[7,8-*h*]quinoline,[1] or benzo[1,2-*h*:3,4-*h*′]diquinoline.[3] Introduction of methoxy groups in positions 2 and 7 is particularly effective in increasing the basicity of 1,8-bis(dimethylamino)naphthalene.

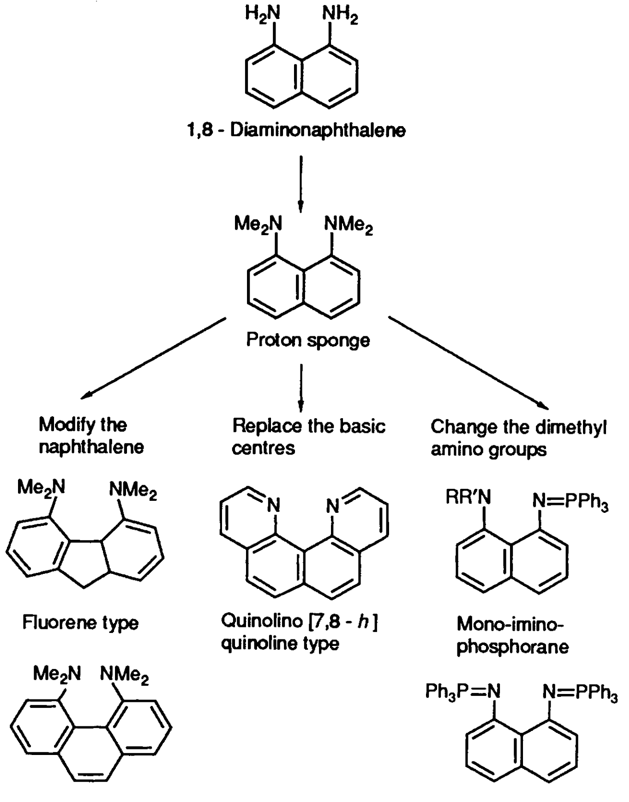

Scheme 1

The extraordinarily high basicity of these compounds [which is also observed in the gas phase, 1,8-bis(dimethylamino)naphthalene being the compound with the highest proton affinity][4] has led to a continuous interest in their properties: mass spectrometry,[5] strain effects on amine basicities[6] and hydrogen bonds in their conjugated acids.[1,7,8] Our experience in the chemistry of iminophosphoranes,[9–11] and the fact that iminophosphoranes are much stronger bases than anilines [*N*,*N*-dimethylaniline, $\mathrm{p}K_\mathrm{a}(\mathrm{CH_3NO_2}) = 11.00$; *N*-phenyliminotriphenylphosphorane, $\mathrm{p}K_\mathrm{a}(\mathrm{CH_3NO_2}) = 16.74$][12] inspired us to develop a new family of 'proton sponges' in which the dimethylamino group has been replaced by an $N{=}P(C_6H_5)_3$ group (Scheme 1).

Since a search of the Cambridge Structural Database[13] (1990 release) revealed that the structure of the parent compound, 1,8-diaminonaphthalene (**1**) had not yet been determined, we decided to study this compound, although it is not a proton sponge [$\mathrm{p}K_\mathrm{a} = 4.61$; *cf.* $\mathrm{p}K_\mathrm{a} = 12.1$ of the bis(dimethylamino) derivative][1] and the mono-iminophosphorane analogue **2** (possibly not a proton sponge either). The dianion of **1** is a useful ligand in coordination chemistry and three such structures have been reported (COYBIB, JAJLUB, VASPUA).[13]

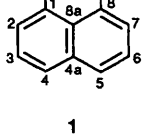

1

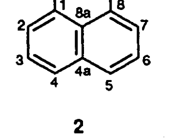

2

Results and Discussion

Chemistry.—Although 1,8-diaminonaphthalene is a commercial product, available in large quantities, it was very difficult to obtain suitable crystals since the compound turns brown on standing. Finally, crystals were obtained by slow evaporation of an ethanol–water solution under an inert atmosphere. They decompose and lose their crystalline character within a few

Table 1 Chemical shift/ppm, coupling constants/Hz and 2D correlations (↭) of compounds 1 and 2 in $CDCl_3$

Compound	Nucleus	1	2	3	4	5	6	7	8	4a	8a	NH_2
1	^1H[a]	—	6.58 $J_{23} = 7.3$	7.18 $J_{34} = 8.1$	7.20 $J_{24} = 1.3$	7.20 $J_{57} = 1.3$	7.18 $J_{56} = 8.1$	6.58 $J_{67} = 7.3$	—	—	—	4.53[b]
			↕	↕	↕	↕	↕	↕				
	^{13}C	144.2	111.3	126.0	119.4	119.4	126.0	111.3	144.2	136.7	116.8	—
2	^1H	—	6.41 $J_{23} = 6.9$	7.12 $J_{34} = 8.0$	6.99 $J_{24} = 1.5$	6.92 $J_{57} = 1.4$	6.78 $J_{56} = 7.9$	6.17 $J_{67} = 7.1$	—	—	—	6.50[b]
			↕	↕	↕	↕	↕	↕				
	^{13}C[c,d]	148.2 $^4J = 1.5$	108.0	126.1	117.8	116.3	125.6	115.2 $^3J = 12.9$	149.4 $^2J = 3.1$	137.8 $^4J = 3.0$	120.3 $^3J = 20.6$	—

[a] These values have been checked with a 600 MHz spectrum. [b] The Ph_3P protons appear at *ca.* 7.66–7.81 (*ortho*) and 7.36–7.54 (*meta* and *para*). [c] ^{13}C–^{31}P coupling constants. [d] Ph_3P carbons appear at (between parentheses the ^{13}C–^{31}P coupling constants): 130.1 (*ipso*)($^1J = 100.0$), 132.6 (*ortho*)($^2J = 9.8$), 128.8 (*meta*)($^3J = 12.1$), 131.9 (*para*)($^4J = 2.6$).

days, but the initial brown colour is due to surface oxidation and does not prevent the determination of the structure. The ^1H and ^{13}C NMR data for compound **1** are given in Table 1. The monoiminophosphorane **2** was prepared from **1** (see the Experimental section) and its NMR characteristics are also reported in Table 1.

NMR Spectroscopy.—The results gathered in Table 1 require some explanation. Particularly useful for the assignment have been the ^{13}C–^{31}P coupling constants of compound **2**. Those of the PPh_3 carbons are similar to other iminophosphorane coupling constants.[10] The coupling constants of the naphthalene carbons are consistent with those of the *N*-phenyl group of the iminophosphorane $Ph–N=PPh_3$, in particular the fact that ^3J(CCNP) is much larger than ^2J(CNP).[14–16]

If one compares the chemical shifts of compounds **1** and **2**, the increments obtained for ^1H and ^{13}C NMR chemical shifts, respectively [$\Delta\delta = \delta(\mathbf{2}) - \delta(\mathbf{1})$] are shown below.

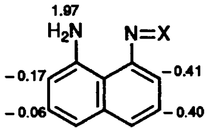

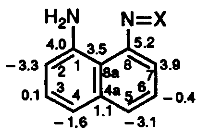

All the CH protons are shifted upfield, whereas the NH protons are strongly shifted in the opposite direction. This is an indication that the intramolecular N–H • • • $N=PPh_3$ hydrogen bond (IMHB) is stronger than the N–H • • • NH_2 one. However, it is necessary to take into account the fact that in compound **1**, the IMHB may involve any one of four protons whereas in compound **2** there are only two available protons. In the ^{13}C NMR spectra, the $\Delta\delta$ values are surprisingly high for remote positions, *e.g.* C-2. We suspect that this large electronic modification affecting carbons C-1, C-2 and C-4 is transmitted partly through the IMHB in compound **2**.

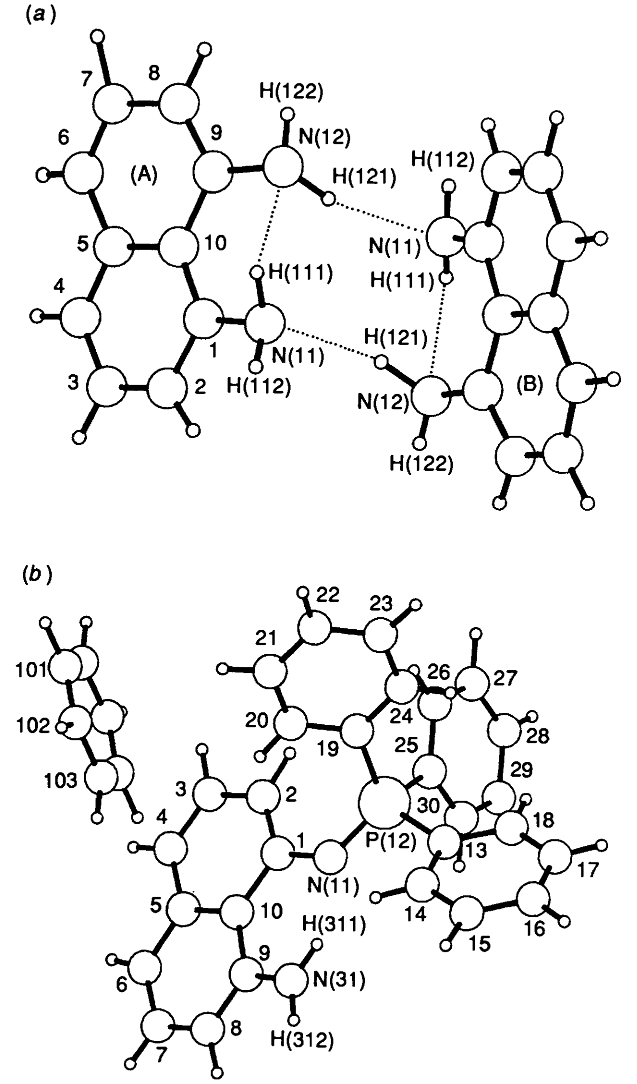

Fig. 1 Molecular structure of (*a*) compound 1 and (*b*) compound 2 with the numbering system adopted in the crystallographic work

X-Ray Crystallography.—Table 2 shows selected geometrical parameters for both compounds, following the numbering system displayed in Figs. 1(*a*) and 1(*b*).[17] The two independent molecules of compound **1** are not significantly different in terms of achieved precision, as tested by a half normal probability plot.[18] The only differences (3 times their pooled standard deviations) appear in the C(1)–C(10)–C(5) and C(5)–C(10)–C(1)–N(11) bond and torsion angles, respectively. However, when the comparison between the two compounds is performed (weighted mean values for compound **1**), the differences concern the asymmetric substitution at the naphthalene moiety (an iminophosphorane group instead of an amino one) that occurs in opposing ways [see Table 2, C(10)–C(1)–N(11) and C(2)–C(1)–N(11)]. This may be due to steric factors which appear to be stronger than those of the hydrogen interaction.

Table 2 Selected geometrical parameters for compounds **1** and **2**. Bond lengths are in Å, and angles in °

	Compound **1**			
	A	B	Optimized[a]	Compound **2**
C(1)–C(2)	1.398(11)	1.379(10)	1.398	1.382(3)
C(1)–C(10)	1.420(7)	1.426(7)	1.447	1.447(3)
C(1)–N(11)	1.417(9)	1.400(8)	1.404	1.392(3)
C(2)–C(3)	1.396(16)	1.394(10)	1.405	1.399(4)
C(3)–C(4)	1.344(18)	1.342(10)	1.370	1.358(4)
C(4)–C(5)	1.398(13)	1.399(10)	1.421	1.409(4)
C(5)–C(6)	1.425(11)	1.415(8)	1.422	1.427(4)
C(5)–C(10)	1.430(10)	1.426(8)	1.422	1.425(3)
C(6)–C(7)	1.331(18)	1.364(12)	1.370	1.353(5)
C(7)–C(8)	1.391(16)	1.394(12)	1.405	1.379(6)
C(8)–C(9)	1.345(9)	1.377(8)	1.398	1.387(3)
C(9)–C(10)	1.426(10)	1.422(10)	1.447	1.442(3)
C(9)–N(12)	1.433(10)	1.398(10)	1.403	1.369(4)
N(11)–P(12)/N(31)	—	—	—	1.575(2)
P(12)–C(13)	—	—	—	1.800(2)
P(12)–C(19)	—	—	—	1.812(2)
P(12)–C(25)	—	—	—	1.811(2)
C(1)–C(10)–C(5)	119.1(5)	116.9(5)	117.4	118.6(2)
C(9)–C(10)–C(5)	116.5(5)	118.0(4)	117.4	117.5(2)
C(10)–C(1)–N(11)	122.4(5)	122.3(5)	122.1	118.4(2)
C(2)–C(1)–N(11)	118.9(5)	118.4(5)	118.5	123.2(2)
C(8)–C(9)–N(12)/N(31)	118.7(7)	120.1(6)	118.5	118.5(2)
C(10)–C(9)–N(12)/N(31)	120.7(5)	120.3(5)	122.2	122.2(2)
C(1)–C(10)–C(9)	124.5(4)	125.1(5)	125.2	123.9(2)
C(1)–N(11)–P(12)	—	—	—	128.5(2)
N(11)–P(12)–C(13)	—	—	—	106.5(1)
N(11)–P(12)–C(19)	—	—	—	115.5(1)
N(11)–P(12)–C(25)	—	—	—	116.2(1)
N(11)–C(1)–C(10)–C(9)	1.5(9)	−4.5(9)	7.0	1.8(3)
N(12)–C(9)–C(10)–C(1)	7.3(9)	−10.0(9)	6.9	6.8(4)
C(5)–C(10)–C(1)–N(11)	−177.8(6)	172.8(6)	−173.0	−177.9(2)
C(5)–C(10)–C(9)–N(12)/N(31)	−173.4(6)	172.8(6)	−173.0	−173.5(2)
C(2)–C(1)–N(11)–P(12)	—	—	—	−2.8(3)

[a] See the text.

Table 3 Deformation/° around C(5)–C(10) and N(11)–P(12) bonds

	Compound **1**			
	A	B	Optimized[a]	Compound **2**
C(4)–C(5)–C(10)–C(1)	−4.4(10)	5.7(9)	−7.7	−2.5(3)
C(6)–C(5)–C(10)–C(1)	173.5(7)	−176.8(6)	172.2	176.0(2)
C(6)–C(5)–C(10)–C(9)	−5.8(10)	4.4(9)	−7.9	−3.4(4)
C(4)–C(5)–C(10)–C(9)	176.3(7)	−173.1(6)	172.2	177.8(2)
C(1)–N(11)–P(12)–C(13)	—	—	—	−173.0(2)
C(1)–N(11)–P(12)–C(19)	—	—	—	72.3(2)
C(1)–N(11)–P(12)–C(25)	—	—	—	−55.0(2)
χ_t	−5.1(4)	5.1(4)	−7.8	−3.1(1)
$\chi_{1.9}$	−3.4(12)	−1.2(11)	−0.1	1.5(6)
$\chi_{6.4}$	0.7(12)	−2.5(11)	−0.1	0.3(4)
χ_t	—	—	—	−51.9(1)
$\chi_{25.13}$	—	—	—	−2.0(3)
$\chi_{25.19}$	—	—	—	−7.3(3)
$\chi_{13.19}$	—	—	—	−5.3(3)

[a] See the text.

This produces deformations of the C(1) substitution angles instead of the C(9) ones.

The naphthalene moiety in both compounds presents a pattern of bond distances and angles similar to those of naphthalene itself.[19] Nevertheless, some distortions from planarity have been observed (see Table 3 and Fig. 2), and these have been analysed by means of the torsion angles around the C(5)–C(10) bond.[20] In all cases, the χ_t parameter has values in the range −5.1(4)° to −3.1(1)° (χ_t measures the twist of the rear-end substituents with respect to the front-end ones and has been corrected for deformations). The deviation from the ideal values of the dihedral angle between two planes with a common edge [*i.e.* C(5)–C(10)–C(1), C(5)–C(10)–C(9)], as measured by the χ_{ij} parameters, tends to be greater at the C(10) end where the substitution takes place than at the C(5) end ($\chi_{1,9} > \chi_{6,4}$). Molecule B in compound **1** is an exception, the individual values, $\chi_{1,9}$ and $\chi_{6,4}$, being just up to three times its standard deviations. In Table 3 we report the deformations around the P=N double bond.

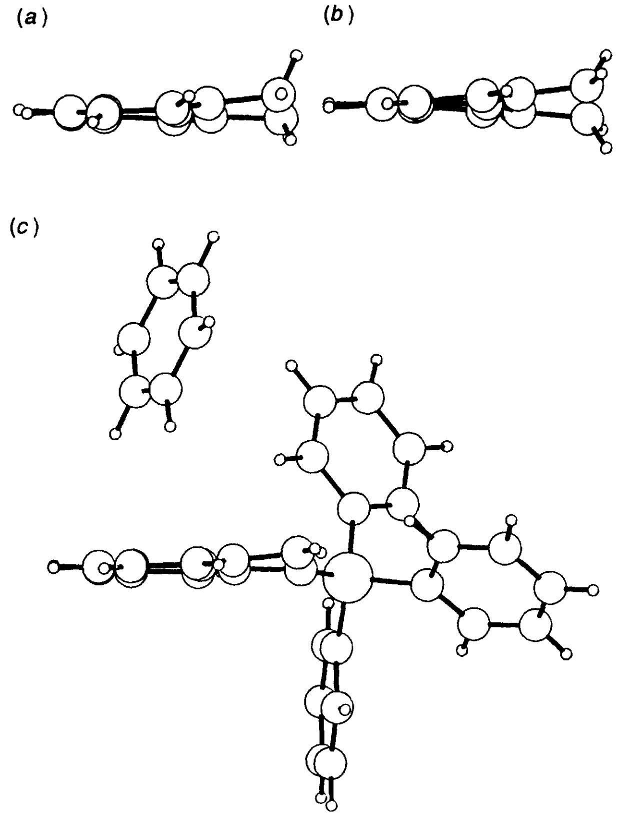

Fig. 2 Perspective view of the molecules showing the naphthalene distortions: (*a*) X-ray data for compound **1**; (*b*) optimized geometry; (*c*) X-ray data for compound **2**

The four N–H atoms of compound **1** exist in four different environments (Table 4) which can be summarized as follows.

	N–H ··· N intramolecular hydrogen bond (IMHB)	N–H ··· N intermolecular hydrogen bond	N–H ··· π with the centroids of the benzene rings	N–H atoms free of interaction
1	H(111A) H(111B)	H(121A) H(121B)	H(112A) H(112B)	H(122A) H(122B)
2	H(311)	—	—	H(312)

The IMHB is significantly shorter and more linear in compound **2** than in compound **1**, an observation which is consistent with the result obtained from NMR studies in solution. The intermolecular contacts involving C–H atoms and the centroids of the fused benzene rings are present in both compounds (Table 4). Moreover, in compound **2**, the solvent benzene molecule and the phenyl rings are also involved in this type of interaction. They are of quasi 'T' type[21] with distances between centroids in the range 4.644(5)–4.932(4) Å and 4.869(2)–5.116(2) Å, for compounds **1** and **2**, respectively.

The benzene guest is included within a hole left by the host matrix of **2**. This hole has been examined[22] to estimate its volume, 215.1 Å^3, and its surface area, 215.2 Å^2; its maximum dimensions being ±4.92, ±4.01, ±3.46 Å around its centroid ($\frac{1}{2}$, 0, 0) (plus the equivalent one in the unit cell). In the same way the benzene guest molecule was examined enabling estimates to be made of its volume, 79.5 Å^3, its surface area, 108.7 Å^2, and its dimensions, ±3.49, ±3.34, ±1.82 Å, centred at the same unit-cell site ($\frac{1}{2}$, 0, 0). The guest molecule is somehow (Fig. 3) misoriented with respect to the principal axis of the matrix hole, the angles between the principal axes of the host and the guest being 22.7, 21.9 and 6.4°, as measured by the angles between the principal axes corresponding to the maximum, medium and minimum dimensions, respectively. Thus, the guest molecule is somehow 'slack' within the hole giving a local packing coefficient $C^{\rm l}_{\rm k} = V(\text{benzene})/V(\text{hole}) = 0.37$ as opposed to the overall value $C^{\rm all}_{\rm k} = [V(\text{host}) + V(\text{guest})]/\text{unit cell volume} = 0.66$. This situation is also reflected in the high value of the thermal coefficients of the

Table 4 Hydrogen interactions. Italics stand for symmetry operations and C(1–10), C(5–10), C(19–24), C(25–30) and C(101–3) for the centroids of the corresponding phenyl rings

	Interatomic distances/Å			
X–H ··· Y	X–H	X ··· Y	H ··· Y	X–H ··· Y/°
(*a*) Compound **1**				
N(11A)–H(111A) ··· N(12A)	1.00(6)	2.716(11)	2.04(6)	123(4)
N(11B)–H(111B) ··· N(12B)	0.85(7)	2.739(10)	2.16(7)	125(5)
N(12A)–H(121A) ··· N(11B)	1.01(–)	3.181(9)	2.20(–)	164(–)
N(12B)–H(121B) ··· N(11A)	1.04(5)	3.315(10)	2.32(5)	160(4)
N(11B)–H(112B) ··· C(1–10B)*i*	0.93(7)	3.614(7)	2.71(7)	167(5)
N(11A)–H(112A) ··· C(1–10A)*ii*	0.85(14)	3.811(8)	3.04(15)	153(11)
C(8A)–H(8A) ··· C(5–10B)*i*	1.02(9)	3.733(10)	3.07(8)	124(5)
C(7B)–H(7B) ··· C(1–10A)*iii*	1.06(6)	3.785(7)	3.03(5)	129(4)
C(6B)–H(6B) ··· C(5–10A)*iii*	1.13(7)	3.596(7)	2.62(7)	144(5)
$i = \frac{1}{2} + x, \frac{1}{2} - y, z$; $ii = -\frac{1}{2} + x, \frac{1}{2} - y, z$; $iii = \frac{1}{2} - x, \frac{1}{2} + y, -\frac{1}{2} + z$				
(*b*) Compound **2**				
N(31)–H(311) ··· N(11)	0.91(3)	2.666(3)	1.95(3)	134(3)
C(102)–H(102) ··· C(1–10)*i*	1.05(7)	3.765(6)	2.94(8)	136(5)
C(29)–H(29) ··· C(1–10)*ii*	1.01(4)	3.683(3)	2.72(4)	160(3)
C(28)–H(28) ··· C(5–10)*ii*	0.95(4)	3.727(3)	2.94(4)	142(2)
C(23)–H(23) ··· C(25–30)*iii*	1.03(3)	3.545(3)	3.08(3)	109(2)
C(21)–H(21) ··· C(101–3)	0.98(4)	3.856(6)	3.05(4)	141(2)
C(17)–H(17) ··· C(19–24)*iii*	0.98(5)	3.701(4)	2.96(4)	133(3)
$i = 1 - x, -y, -z$; $ii = -x, -y, -z$; $iii = \frac{1}{2} - x, \frac{1}{2} + y, \frac{1}{2} - z$				

Table 5 Crystal analysis parameters at room temperature

	1	2
Crystal data		
Formula	$C_{10}H_{10}N_2$	$C_{28}H_{23}N_2P{\cdot}0.5(C_6H_6)$
Crystal habit	Brown prism	Brown prism
Crystal size/mm	0.43 × 0.23 × 0.10	0.33 × 0.23 × 0.17
Symmetry	Orthorhombic, *Pna*2_1	Monoclinic, *P*2_1/*n*
Unit-cell determination:	Least-squares fit from 49 reflections ($\theta < 45°$)	Least-squares fit from 67 reflections ($\theta < 45°$)
Unit cell dimension/Å, °	a = 8.7970(4)	a = 17.6217(10)
	b = 15.7797(8)	b = 11.9629(4)
	c = 12.1189(6)	c = 12.5270(5)
	90, 90, 90	90, 109.532(4), 90
Packing: V/Å, Z	1682.3(1), 8	2488.8(2), 4
D_c/g cm^{-3}, M, F(000)	1.249, 158.202, 672	1.221, 457.534, 964
μ/cm^{-1}	5.612	11.141
Experimental data		
Technique	Four circle diffractometer: Philips PW1100 Bisecting geometry Graphite-oriented monochromator: CuKα $\omega/2\theta$ scans, scan width: 1.5° Detector apertures 1 × 1°, up θ_{max} 65° 1 min per reflection	
Number of reflections:		
Measured	1654	4716
Independent	1482	4232
Observed	1039 [3σ(I) criterion]	3546 [3σ(I) criterion]
Standard reflections:	2 reflections every 90 min No variation	
Solution and refinement		
Solution	Direct methods	
Refinement	Full matrix least-squares on F_0	
Parameters		
Number of variables	292	411
Degrees of freedom	747	3135
Ratio of freedom	3.6	7.6
H atoms	Difference synthesis	
Final shift/error	0.06	0.04
Weighting scheme	Empirical as to give no trends in $\langle w\Delta^2F\rangle$ *vs.* $\langle\lvert F_{obs}\rvert\rangle$ and $\langle\sin\theta/\lambda\rangle$	
Max. thermal value	U22 [C(3A)] = 0.173(9) Å^2	U22 [C(102)] = 0.205(7) Å^2
Final ΔF peaks	0.16 e Å^{-3}	0.16 e Å^{-3}
Final R and R_w	0.053, 0.051	0.045, 0.051
Computer and programs	Vax 6410, XRAY80,[26] SIR88,[27] PESOS,[28] PLUTO[17]	
Scattering factors	*Int. Tables for X-Ray Crystallography*[29]	

Table 6 Final atomic coordinates for compound **1**

	Molecule A			Molecule B		
Atom	x	y	z	x	y	z
C(1)	0.4718(6)	0.2153(3)	0.2500	0.5292(5)	0.3226(3)	−0.1355(6)
C(2)	0.4855(9)	0.2532(6)	0.3538(9)	0.4825(7)	0.2746(4)	−0.2244(7)
C(3)	0.5642(12)	0.2127(9)	0.4388(9)	0.3677(7)	0.3018(5)	−0.2953(7)
C(4)	0.6240(11)	0.1351(8)	0.4243(8)	0.3006(6)	0.3772(5)	−0.2791(7)
C(5)	0.6143(7)	0.0935(4)	0.3227(7)	0.3421(5)	0.4280(3)	−0.1895(6)
C(6)	0.6705(8)	0.0096(6)	0.3082(10)	0.2743(7)	0.5088(4)	−0.1777(7)
C(7)	0.6530(10)	−0.0312(6)	0.2129(12)	0.3170(7)	0.5611(4)	−0.0936(8)
C(8)	0.5906(8)	0.0109(4)	0.1227(9)	0.4201(7)	0.5328(4)	−0.0144(8)
C(9)	0.5434(6)	0.0918(3)	0.1290(7)	0.4841(6)	0.4533(3)	−0.0196(7)
C(10)	0.5416(5)	0.1352(3)	0.2322(6)	0.4531(5)	0.4003(3)	−0.1118(6)
N(11)	0.3930(7)	0.2591(5)	0.1655(8)	0.6517(6)	0.2934(4)	−0.0723(6)
N(12)	0.4879(7)	0.1321(4)	0.0309(6)	0.5788(6)	0.4249(4)	0.0654(7)

benzene molecule. The 'slackness' is not sufficient to allow anything of radius greater than 1.4 Å to be included within the crystal in addition to the already present benzene guest. The maximum dimensions of the cavity in which the benzene molecule is situated, compare well to those obtained from the geometry of the molecule, taking into account the step of 0.2 Å used.

Theoretical Calculations.—Starting from the solid state geometry of compound **1**, an optimization has been carried out

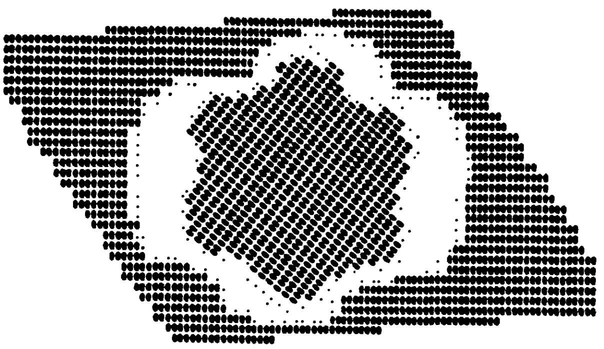

Fig. 3 Section, perpendicular to the lowest hole/guest dimension through the common centroid. This shows how the guest is misoriented with respect to the hole (see the text), but it is also apparent how both follow the same shape.

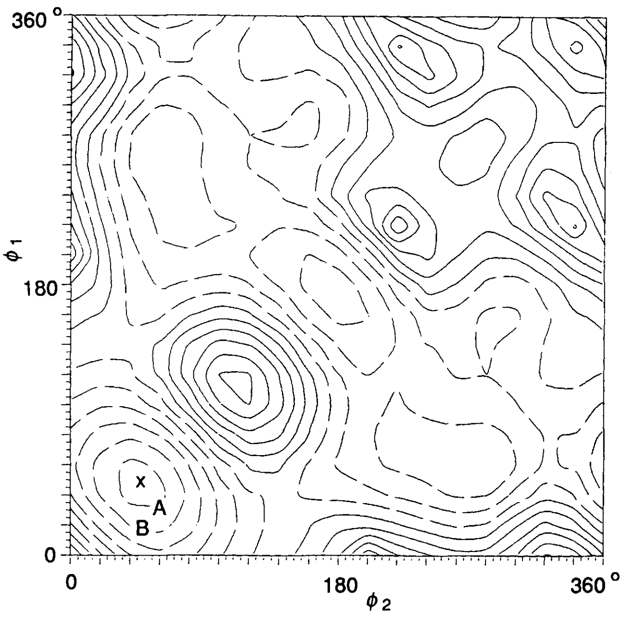

Fig. 4 Potential energy surface, ϕ_1 = C(10)–C(1)–N(11)–H(111) and ϕ_2 = C(10)–C(9)–N(12)–H(121). X stands for the absolute minimum, while A and B stand for the crystallographic conformation found in molecules A and B of compound **1**. Contour lines are separated by 1 kcal mol^{-1}, the full ones correspond to high energies and the dashed ones to low energies.

using the semiempirical method AM1 implemented in the AMPAC series of programs.[23] The isolated molecule displays a binary axis along the C(5)–C(10) bond, a greater χ_t value, and a greater distance between the NH$_2$ groups, resulting in less favourable IMHB geometry than in the crystalline state [N(11) ··· N(12) = 2.822 Å *vs.* 2.716(11) and 2.739(10) Å for molecules A and B, respectively (see also Table 3)].

1,8-Disubstituted naphthalene derivatives show the so-called '*peri*' interaction effect, due to the proximity of the substituents.[24] This effect pushes the amino groups apart and is partly counterbalanced by the intramolecular hydrogen bond. The fact that the calculations slightly underestimate the strength of the IMHB could be due either to the theoretical approximation used or to the fact that in the solid state there are other interactions involving the N–H atoms of compound **1** (see above).

The potential energy surface, Fig. 4,[25] has been calculated as a function of the torsion angles ϕ_1 [C(10)–C(1)–N(11)–H(111)] and ϕ_2 [C(10)–C(9)–N(12)–H(121)] using the optimized geometry as the starting point and a grid of points separated by 20° (190 points in the asymmetric unit). The lowest minimum appears at $\phi_1 = \phi_2 = 47.0°$, compared with the experimental geometries of ϕ_1 = 32(3), 16(5)° and ϕ_2 = 57(3) and 49(3)° for molecules A and B, respectively. A similar map, although less symmetrical, was obtained when the X-ray geometry was used (lowest minimum at ϕ_1 = 48.5° and ϕ_2 = 45.3°). In conclusion, the experimental geometry of 1,8-diaminonaphthalene in the solid state roughly corresponds to the conformation of minimum energy.

Table 7 Final atomic coordinates for compound **2**

Atom	*x*	*y*	*z*
C(1)	0.192 8(1)	0.060 8(2)	−0.074 8(2)
C(2)	0.221 4(1)	−0.018 1(2)	0.009 7(2)
C(3)	0.230 9(2)	−0.130 3(2)	−0.014 5(2)
C(4)	0.210 8(2)	−0.165 5(2)	−0.123 6(3)
C(5)	0.179 4(1)	−0.090 4(2)	−0.214 2(2)
C(6)	0.153 9(2)	−0.129 4(3)	−0.328 4(3)
C(7)	0.121 7(2)	−0.057 9(3)	−0.415 5(3)
C(8)	0.115 6(2)	0.054 7(3)	−0.395 9(2)
C(9)	0.141 6(1)	0.099 1(2)	−0.287 3(2)
C(10)	0.171 3(1)	0.025 0(2)	−0.191 5(2)
N(11)	0.182 3(1)	0.172 8(2)	−0.053 2(1)
P(12)	0.195 79(3)	0.231 53(4)	0.064 28(4)
C(13)	0.159 9(1)	0.372 7(2)	0.033 3(2)
C(14)	0.175 7(2)	0.428 8(2)	−0.054 1(3)
C(15)	0.152 7(3)	0.539 4(3)	−0.076 2(3)
C(16)	0.114 8(2)	0.594 7(3)	−0.011 6(4)
C(17)	0.100 0(2)	0.540 6(3)	0.075 1(4)
C(18)	0.122 2(2)	0.429 2(2)	0.098 4(3)
C(19)	0.299 9(1)	0.248 3(2)	0.153 3(2)
C(20)	0.359 9(1)	0.198 0(2)	0.121 5(2)
C(21)	0.440 2(1)	0.217 4(3)	0.184 8(2)
C(22)	0.460 3(1)	0.285 3(3)	0.278 4(2)
C(23)	0.400 7(1)	0.335 3(2)	0.310 5(2)
C(24)	0.320 7(1)	0.317 4(2)	0.247 6(2)
C(25)	0.141 9(1)	0.172 5(2)	0.151 2(2)
C(26)	0.178 8(1)	0.138 3(2)	0.262 5(2)
C(27)	0.133 0(2)	0.096 9(2)	0.324 4(2)
C(28)	0.050 4(2)	0.089 5(3)	0.276 0(2)
C(29)	0.013 3(2)	0.122 0(3)	0.165 6(2)
C(30)	0.058 9(1)	0.163 0(2)	0.103 0(2)
N(31)	0.138 9(1)	0.212 6(2)	−0.275 0(2)
C(101)	0.551 7(4)	0.071 9(8)	−0.023 2(8)
C(102)	0.580 2(3)	0.004 1(8)	0.062 1(7)
C(103)	0.528 2(5)	−0.070 1(7)	0.087 7(7)

It is at present practically impossible to carry out similar calculations on compound **2**, owing to both the number of atoms and the torsion angles.

Experimental

M.p.s were determined with a Kofler hot-stage microscope and are uncorrected. Spectral studies were performed with the following instruments: IR, Nicolet FT-5DX; ^{1}H and ^{13}C NMR, Bruker AC-200 all chemical shifts expressed in ppm relative to SiMe$_4$); MS (70 eV), Hewlett-Packard 5993C. Combustion analyses were performed with a Perkin-Elmer 240C instrument.

Crystal-structure Determination of Compounds **1** *and* **2**.—The crystallographic analysis is summarized in Table 5. The final atomic coordinates are presented in Tables 6 and 7. The two independent molecules in compound **1** are related by a pseudo-symmetry centre at (0.4934, 0.2645, 0.0601), the maximum deviations being due to the *x* coordinates. The benzene solvate molecule, compound **2**, is located at a crystallographic symmetry centre.*

---

* *Supplementary data* (see 'Instructions for Authors (1991)', *J. Chem. Soc., Perkin Trans. 2*, 1991, January issue). Thermal parameters, hydrogen-atom coordinates and bond distances have been deposited at the Cambridge Crystallographic Data Centre.

1-Amino-8-triphenylphosphoranylideneaminonaphthalene (**2**).—Bromine (3.19 g, 20 mmol) in dry benzene (30 cm^3) was added to a stirred solution of triphenylphosphine (5.24 g, 20 mmol) in the same solvent (50 cm^3) at 0–5 °C under nitrogen. The mixture was stirred for 1 h and then allowed to warm to room temperature. A solution of **1** (1.58 g, 10 mmol) and triethylamine (4.05 g, 40 mmol) in dry benzene (50 cm^3) was added. The reaction mixture was refluxed for 12 h and after cooling, the separated solid was collected by filtration, washed with cold water, air-dried and passed on an Amberlite-400 (OH) column, eluting with ethanol to give **2** in 67% yield as yellow crystals, m.p. 163–164 °C (decomp.) (Found: C, 81.55; H, 5.7; N, 5.9. $C_{28}H_{23}N_2P\cdot0.5C_6H_6$ requires: C, 81.38; H, 5.73; N, 6.12); ν_{max}(Nujol)/cm^{-1} 3449vs, 3233vs, 1568vs, 1438vs, 1309vs, 1276s, 1103s, 1086s, 1070s, 945m, 813m, 757m, 737m, 717s and 694s; *m/z* (%) 418 (M$^+$) (1), 218 (53), 217 (100), 216 (76), 186 (34), 183 (97), 155 (19) and 130 (16).

Acknowledgements

The assistance of Prof. F. H. Cano is gratefully acknowledged. Financial support was provided by the *Dirección General de Investigación Científica y Técnica* (Project Nos. PB-0291 and PB87-0094-CO2-00).

References

1 H. A. Staab and T. Saupe, *Angew. Chem., Int. Ed. Engl.*, 1988, **27**, 865.
2 H. Staab, M. Höne and C. Krieger, *Tetrahedron Lett.*, 1988, **29**, 1905.
3 H. A. Staab, M. A. Zirnstein and C. Krieger, *Angew. Chem., Int. Ed. Engl.*, 1989, **28**, 86.
4 R. W. Taft, *Prog. Phys. Org. Chem.*, 1983, **14**, 247.
5 M. Rentzea, T. Saupe, W. Brox and H. A. Staab, *Org. Mass Spectrom.*, 1989, **24**, 367.
6 R. W. Alder, *Chem. Rev.*, 1989, **89**, 1215.
7 Z. Pawelka and Th. Zeegers-Huyskens, *J. Mol. Struct.* (*Theochem.*), 1989, **200**, 565.
8 Z. Malarski, T. Lis, E. Grech, J. Nowicka-Scheibe and K. Majewska, *J. Mol. Struct.*, 1990, **221**, 227.
9 P. Molina, M. Alajarín, J. R. Saez, M. C. Foces-Foces, F. H. Cano, R. M. Claramunt and J. Elguero, *J. Chem. Soc., Perkin Trans. 1*, 1986, 2037.
10 P. Molina, M. Alajarín, C. L. Leonardo, R. M. Claramunt, M. C. Foces-Foces, F. H. Cano, J. Catalán, J. L. G. de Paz and J. Elguero, *J. Am. Chem. Soc.*, 1989, 111, 355.
11 R. M. Claramunt, M. C. Foces-Foces, F. H. Cano, A. Fruchier, P. Molina, M. Alajarín, C. L. Leonardo and J. Elguero, *J. Chem. Soc., Perkin Trans. 2*, 1990, 1859.
12 Yu. G. Gololobov, I. N. Zhmurova and L. F. Kasukhin, *Tetrahedron*, 1981, **37**, 437.
13 F. H. Allen, S. Bellard, M. D. Brice, B. A. Cartwright, A. Doubleday, H. Higgs, T. Hummelink, B. G. Hummelink-Peters, O. Kennard, W. D. S. Motherwell, J. R. Rogers and D. G. Watson, *Acta Crystallogr., Sect. B*, 1979, **35**, 2331.
14 T. A. Albright, W. J. Freeman and E. Schweizer, *J. Org. Chem.*, 1976, **41**, 2716.
15 H. Fritz and C. D. Weis, *J. Org. Chem.*, 1978, **43**, 4900.
16 M. Pomerantz, D. S. Marynick, K. Rajeshwar, W. N. Chou, L. Throckmorton, E. W. Tsai, P. C. Y. Chen and T. Cain, *J. Org. Chem.*, 1986, **51**, 1223.
17 W. D. S. Motherwell, PLUTO, *A Program for Plotting Crystal and Molecular Structures*, Cambridge University, England, 1978.
18 G. A. Abrahams and E. T. Keve, *Acta Crystallogr., Sect. A*, 1971, **27**, 157.
19 C. P. Brock and J. D. Dunitz, *Acta Crystallogr., Sect. B*, 1982, **38**, 2218.
20 F. H. Cano, C. Foces-Foces and S. García-Blanco, *J. Cryst. Mol. Struct.*, 1979, **9**, 107.
21 G. R. Desiraju, *Crystal Engineering*, Elsevier, Amsterdam, 1989.
22 M. Martinez-Ripoll, F. H. Cano and C. Foces-Foces, Program HOLES, to be published. We divide the whole unit cell into celldets of 0.2 Å in size, deciding if any of them are within the reach of the van der Waals radius of any atom of the host matrix or not (that one being a hole celldet) and then smoothing down the clefts in the limits of the hole by rolling on the surface a ball of 1.4 Å in radius to obtain the final hole definition.
23 *QCPE*, Program No. 527: AMPAC version 2.01, Indiana University, USA.
24 V. Balasubramaniyan, *Chem. Rev.*, 1966, **66**, 507.
25 Precision Visuals DI3000 V5.09, Boulder, Colorado, 80301, USA, 1987.
26 J. M. Stewart, P. A. Machin, C. W. Dickinson, H. L. Ammon, H. Heck and H. Flak, *The X-Ray System*, Technical Report TR-446, Computer Science Center, University of Maryland, USA, 1976.
27 M. C. Burla, M. Camalli, G. Cascarano, C. Giacovazzo, G. Polidori, R. Spagna and D. Viterbo, 'SIR88', *J. Appl. Crystallogr.*, 1989, **22**, 389.
28 M. Martinez-Ripoll and F. H. Cano, *PESOS*, unpublished program.
29 *International Tables for X-Ray Crystallography*, Kynoch Press, Birmingham, England, 1974, vol. IV.

Paper 0/05746K
Received 21*st December* 1990
Accepted 13*th February* 1991